

Interaction Note

Note 615

April 2011

In-Flight versus Ground-Test Lightning Interactions in Composite Airframes
Effects of External vs. Internal inductance
An Errata to Everything Previously Published

Larry West
10215 Beechnut St, Suite 1003
Houston, TX 77072

abstract

Indirect lightning waveforms have been derived from system level ground-testing of aircraft with the $1.5\mu\text{s}/88\mu\text{s}$ double exponential Component A current with a well defined current return path in proximity to the system under test that defines the external inductance of the system and its conductors. In-flight, there is no current return path and the inductances of the system and its conductors are self or internal inductances which are smaller by x100 than the external inductance in the ground tests.

All design allocations and box testing that heretofore called out cable current Waveform 5A (WF5A) will have to be changed to WF4 and increased. System level test results containing WF5A cable currents will have to be ignored for certification purposes and only be used for model verification and checking groundplane and cable shield integrity or be extrapolated by the electrical parameters of the skin, groundplanes, and cables. Shielding the WF4 current has the same problems as WF5A since WF5A is the late time low frequency portion of WF4. More high frequency current passes through the interior conductors of composite airframes including lightning strike Component A, above, and the faster rise time Components D and H. Components A, D, and H all excite the same peak levels of WF2 and WF3 within x2 or 6dB.

There is no present-day system level ground test of in-flight interactions described herein although several options are under study.

1. Visualization, In-Flight vs. Ground Test

Lightning interaction with a composite airframe in-flight versus in a ground test presents is illustrated in Figures 1 and 2. The indirect lightning I-R-drop WF5A cable current waveform has been derived from ground test data where the external inductance controls the waveforms. In-flight, with no ground plane or controlled current return path, the internal inductance controls the waveforms. The difference between the two is about x100 for applicable airframes and cable shield geometries. The electrical parameters are derived in Section 2.

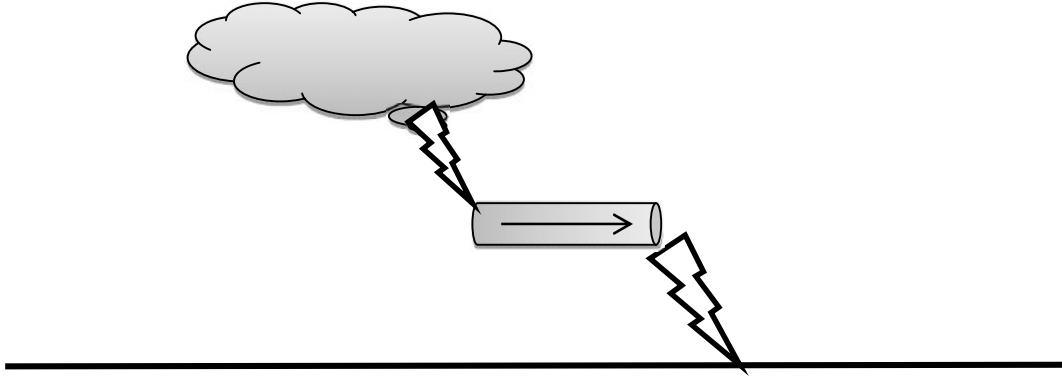


Figure 1. Lightning One Way Current Flow with No Return Circuit, No External Inductance

Typical example results for a carbon fiber composite (CFC) cylinder with 10m length, 2m radius, 2mm thickness, and $\sigma = 10^4$ S/m: (See Section 2.)

- (1) $L \equiv L_{internal} = \frac{\mu_0 \cdot l}{4 \cdot \pi} \cdot \frac{t}{b} = 1nH$
- (2) $R_{dc} = \frac{l}{2 \cdot \pi \cdot b \cdot t \cdot \sigma} = 80m\Omega$
- (3) $\frac{L_{int}}{R_{dc}} = 100ns$

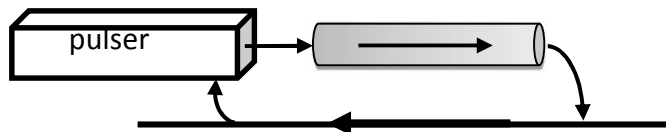


Figure 2. Lightning Ground Test with Return Circuit, External inductance

Typical example results for same cylinder in a ground test with a nearby return current is:

- (4) $L \equiv L_{external} = \frac{\mu_0 \cdot l}{2 \cdot \pi} \cdot \ln\left(\frac{2 \cdot h}{b}\right) = 500nH \gg L_{internal}$
- (5) $\frac{L_{ext}}{R_{dc}} \cong 69\mu s \gg \frac{L_{int}}{R_{dc}}$

The lower internal inductances of the in-flight case render the current division between the aircraft skin and its internal conductors (routed parallel to the lightning current) mostly resistive. The higher external inductances in the system level ground test redistribute the currents quite differently, the early time part of the lightning transient traversing the skin and the late time traversing the interior cables. The high inductance in the ground test, above, creates Waveform 5A currents on cables.

2. Derivation of System Electrical parameters

The division of current between a vehicle's composite skin and its internal conductors' is dependent upon the resistance and inductance of the two as depicted in the heuristic model in Figure 3.¹ The long wavelengths of lightning relative to the size of aerospace vehicles renders a simple RL circuit adequate at this level of system application. The cable current waveform has been derived from ground tests with a well defined nearby current return path. In-flight, there is no current return path. The difference between the two is the inductance of the conductors, external versus internal inductance as explained below.

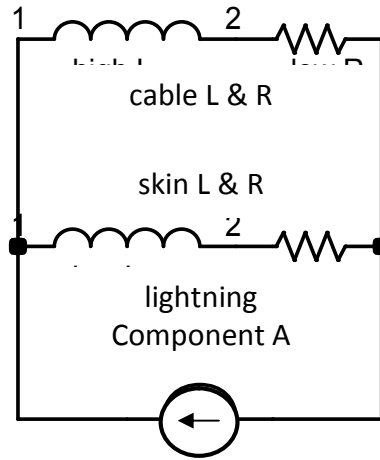


Figure 3. Heuristic RL Model of Composite Skin and Metallic Conductors

The cable current in this model is given by the following expression:

$$(1) \quad I_{cable}(s) = I_A(s) \cdot \frac{Z_{CFC}(s)}{Z_{CFC}(s) + Z_{cable}(s)} = I_A \cdot \left(\frac{1}{s+\alpha} - \frac{1}{s+\beta} \right) \cdot \frac{L_{CFC}}{L_{CFC} + L_{cable}} \cdot \frac{s+b}{s+\gamma}, \text{ where}$$

$$(2) \quad I_A \cong 218 \text{ kA} \text{ in order to obtain a 200 kA peak time domain value of Component A,}$$

$$(3) \quad \alpha^{-1} \cong 88 \mu\text{s}, \text{ the lightning Component A decay time,}$$

$$(4) \quad \beta^{-1} \cong 1.5 \mu\text{s}, \text{ the lightning Component A rise time,}$$

$$(5) \quad Z_{CFC} = R_{CFC} + s \cdot L_{CFC}, \text{ the impedance of the composite CFC skin,}$$

$$(6) \quad Z_{cable} = R_{cable} + s \cdot L_{cable}, \text{ the impedance of one cable,}$$

$$(7) \quad b^{-1} = L_{cable}/R_{cable}, \text{ the L/R time constant of the cable, and}$$

$$(8) \quad \gamma^{-1} = (L_{CFC} + L_{cable})/(R_{CFC} + R_{cable}), \text{ the loop time constant of the CFC skin and cable, a result of the parallel RL circuit branches and the current source.}^1$$

The electrical parameters will be derived next.

2.1. Resistance and Inductance of a Cylinder

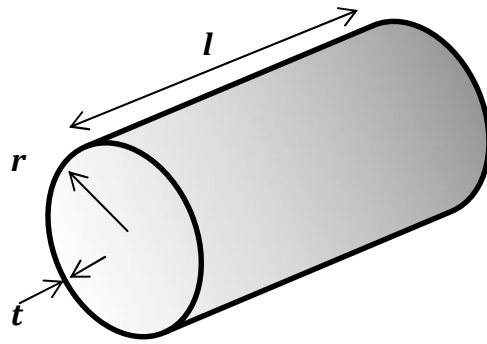


Figure 4. Cylindrical Shell Geometric Parameters
Cylindrical skin of length l , radius r , skin thickness t , and conductivity σ

2.1.1 Resistance

The DC resistance of finite length cylindrical shells is estimated as follows:^{2,3}

$$(9) \quad R_{dc} = \frac{l}{2 \cdot \pi \cdot r \cdot t \cdot \sigma}.$$

Although we seldom have a need for the high frequency AC resistance, it is as follows:

$$(10) \quad R_{ac} = \frac{l}{2 \cdot \pi \cdot r \cdot \delta \cdot \sigma}, \text{ where}$$

$$(11) \quad \delta = \sqrt{1 / \pi \cdot f \cdot \sigma \cdot \mu} \text{ is the material skin depth.}$$

An in-flight aerospace vehicle is isolated with respect to ground and any return circuit in free space therefore its inductance is its internal inductance. When struck by lightning, the vehicle has a high impedance current source and sink attached at either end.

We never deal with solid continuous wires or cylinders but rather twisted strands of smaller wires or woven carbon filament with one or more contra-woven layers on top of another. Newer CFC vehicle skin even has wires woven in with the CFC weave for direct strike lightning protection. Also, newer metal plated composite braid shields also have metal wires woven in with the plated composite fiber weave for slightly better shielding.

2.1.2. Inductance

Since we can't find a good physics write up anywhere else, the lightning interaction offers a good place to differentiate between different kinds of inductance and apply them.

Self or internal inductance is the inductance of a conductor in free space meaning not interacting with another conductor through their external magnetic fields. It only "interacts", if you will, with its own magnetic field within the conductor. It's a characteristic of all conductors independent of their surroundings or, more pointedly, independent of other conductors, their currents, and their magnetic

fields. It is best determined by self impedance solutions to the conductors' boundary value problem. See Figure 5.

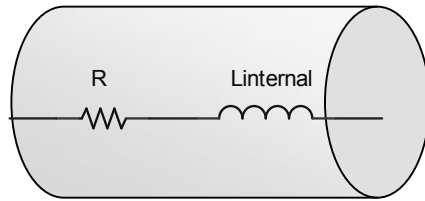


Figure 5. Equivalent Internal Electrical Parameters, R_{int} & L_{int} , of a Conducting Element

External inductance is the inductance of a closed loop or closed circuit that interacts with itself through its own magnetic field created within the loop as in Figure 6. A loop antenna, a transmission line, or any circuit carrying current generated by its own power source and returning to the power source are examples of the effect of a return current closing a circuit. It is best determined by a flux-linkage model. Many definitions do not include the closed circuit concept although it's tacitly assumed in image theory.

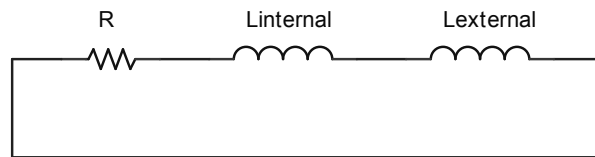


Figure 6. Closed Circuit or Transmission Line with L_{int} & L_{ext}

Mutual inductance is the inductance between two closed circuits that comes from the magnetic field of one passing through the other and vice versa as in Figures 7 and 8. It is best determined by a flux-linkage model.

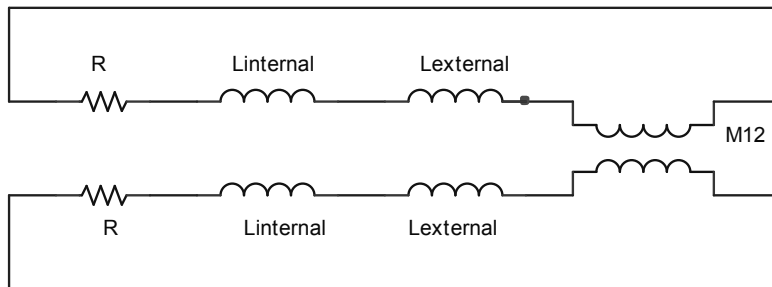
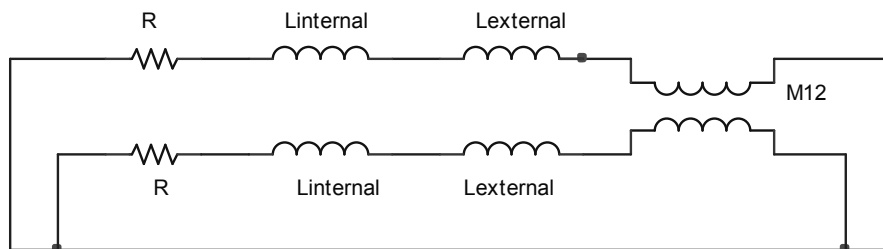


Figure 7. Two Separate Closed Circuits or Transmission Lines with L_{int} , L_{ext} , & M_{12}



**Figure 8. Two Closed Circuits with Common Ground/Return & L_{int} , L_{ext} , & M_{12}
A Common Occurrence for Grounded Shielded Cables**

Common mode & differential mode currents in a system of parallel conductors conducting parallel lightning currents on different conductors with different impedances forces us to use both internal

and external and/or mutual inductances as depicted in Figure 9. Common mode currents are prevalent in a system struck by lightning. These will have internal impedances. Different conductors with different individual impedances will conduct different currents that can be divided into common mode (sum) and differential mode (difference) currents. We will explain that the common mode currents are controlled by internal impedances and differential mode currents are controlled by external impedances and mutual inductance.

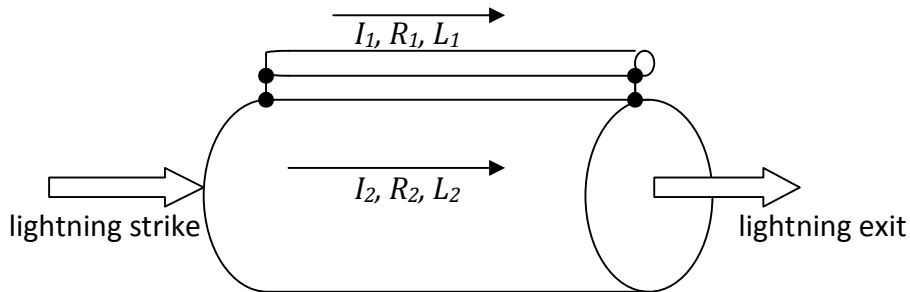


Figure 9. Raceway or Wing Spar Cable alongside Structure

Let's look at two parallel conductors in the lightning path with different internal impedances which means that they conduct different currents, I_1 and I_2 :

(12) $I_{cm} \equiv I_1 + I_2$, the common mode (sum) current and

(13) $I_{dm} \equiv I_1 - I_2$, the differential mode (difference) current.

Each conductor will mutually magnetically couple to the other and induce a voltage in series within the conductors.

(14) $V_2 = -i\omega \cdot M_{21} \cdot I_1$ and

(15) $V_1 = -i\omega \cdot M_{12} \cdot I_2$.

(16) $M_{12} = \frac{\mu_0 \cdot l}{2 \cdot \pi} \cdot \ln\left(\frac{d-r_2}{r_1}\right)$, where d is the conductor separation, center-to-center, r_1 is the radius of conductor #1, and r_2 is the radius of conductor #2. Because the conductors are different sizes, the mutual inductance is not symmetric, i.e.

(17) $M_{21} = \frac{\mu_0 \cdot l}{2 \cdot \pi} \cdot \ln\left(\frac{d-r_1}{r_2}\right) \neq M_{12}$.

As an example, for $r_1 = 1\text{m}$, $r_2 = 1\text{cm}$, and $d = 1.2\text{m}$, $M_{21}/M_{12} \approx 69$.

We now have a differential voltage in the closed circuit path of the two conductors:

(16) $V_{dm} = -i\omega \cdot (M_{21} \cdot I_1 - M_{12} \cdot I_2)$.

We have several configurations in aerospace vehicles where this differential mode excitation with external inductances is important, notably raceway cables and wing spar cables.

2.1.2.1. Grover and Rosa, Internal Inductance^{6,7,8}

The finite-length bodies modeled by Rosa and Grover^{6,7,8}, have inductances proportional to the following:

$$(10) \quad L_{internal} \approx \frac{\mu_0}{2 \cdot \pi} l \cdot \left[\ln\left(\frac{2 \cdot l}{R}\right) - \mathbf{1} \right].$$

This author takes issue with Grover's model formulas because they do not scale with length correctly, in this case, the inductance per unit length scaling to infinity instead of a finite value. Also, Grover's shallow discussion of cylindrical shells leaves some doubt about his methods and rigor.

2.1.2.2. Schelkunoff: Internal Impedance²

Internal impedance including resistance and inductance is derived from the ratio of an electric field, E_s , on the surface of a conductor to the current, I , within the conductor:^{2,3}

$$(11) \quad Z'_{int} = \frac{E_s}{I}$$

The current density, J , and fields are all solutions of the same equation inside the conductor:

$$(12) \quad \nabla^2 \vec{J} = i\omega \cdot \mu \cdot \sigma \cdot \vec{J} = k^2 \cdot \vec{J}$$

which derive from Maxwell's equations inside the conductor:

$$(13) \quad \nabla \times \vec{H} = \sigma \cdot \vec{E} \text{ and}$$

$$(14) \quad \nabla \times \vec{E} = i\omega \cdot \mu \cdot \vec{H} \text{ and}$$

$$(15) \quad \vec{J} = \sigma \cdot \vec{E}.$$

The electrical phenomenon within a conductor is characterized and controlled by the very low field impedance, $\sigma \cdot E \ll H$ over a large frequency range.

In cylindrical coordinates, the current density, J , solution to the boundary value problem boils down to a sum of appropriate Bessel functions, for example:

$$(16) \quad J(k \cdot r) = A \cdot J_0(k \cdot r) + B \cdot N_0(k \cdot r)$$

Where $J_0(k \cdot r)$ is a Bessel function of the first kind and zero order, $N_0(k \cdot r)$ is a Bessel function of the second kind and zero order, and $k \cong \sqrt{i\omega \cdot \mu \cdot \sigma}$, assuming $\sigma \cdot E \gg \omega \cdot \epsilon_0 \cdot E$.

For a solid cylinder³ of length, l ,

$$(17) \quad Z_{int} \cong \frac{k \cdot l}{2 \cdot \pi \cdot r \cdot \sigma} \cdot \frac{J_0(kr)}{J'_0(kr)}.$$

At lower frequencies, when $\delta > 2 \cdot r$, a solid cylinder has an internal impedance

$$(18) \quad Z_{int} \cong \frac{l}{\pi \cdot r^2 \cdot \sigma} + i\omega \cdot \frac{\mu_0 \cdot l}{8 \cdot \pi}$$

At higher frequencies where $\delta < 2 \cdot r$ and the skin depth is defined as

$$(19) \quad \delta = \sqrt{1/\pi \cdot f \cdot \mu \cdot \sigma},$$

$$(20) \quad Z_{int} \cong \frac{l}{2 \cdot \pi \cdot r \cdot \delta \cdot \sigma} + i\omega \cdot \frac{\mu_0 \cdot l}{4 \cdot \pi} \cdot \frac{\delta}{r}$$

Schelkunoff's solution for the internal impedance of a cylindrical shell is given by the following approximation graphed in Figure 5, below:

$$(21) \quad Z_{int}(\omega) \cong R_{dc} \cdot \sqrt{i\omega \cdot \tau_d} \cdot \coth \sqrt{i\omega \cdot \tau_d}, \text{ where}$$

$$(22) \quad \tau_d = \mu \cdot \sigma \cdot t^2, \text{ the diffusion time through a thickness, } t.$$

Using this model a cylindrical shell of radius, b , and thickness, t , has a low frequency resistance and inductance as follows:

$$(22) \quad R_{int} \cong \frac{l}{2 \cdot \pi \cdot b \cdot t \cdot \sigma}$$

$$(23) \quad L_{int} \cong \frac{\mu_0 \cdot l}{4 \cdot \pi} \cdot \frac{t}{b}$$

The high frequency internal resistance and inductance are as follows:

$$(24) \quad R_{int} \cong \frac{l}{2 \cdot \pi \cdot b \cdot \delta \cdot \sigma} \text{ and}$$

$$(24) \quad L_{int} \cong \frac{\mu_0 \cdot l}{4 \cdot \pi} \cdot \frac{\delta}{b}, \text{ both the same as a solid cylinder of the same radius, (20).}$$

Internal Impedance, 36AWG Braid Shield

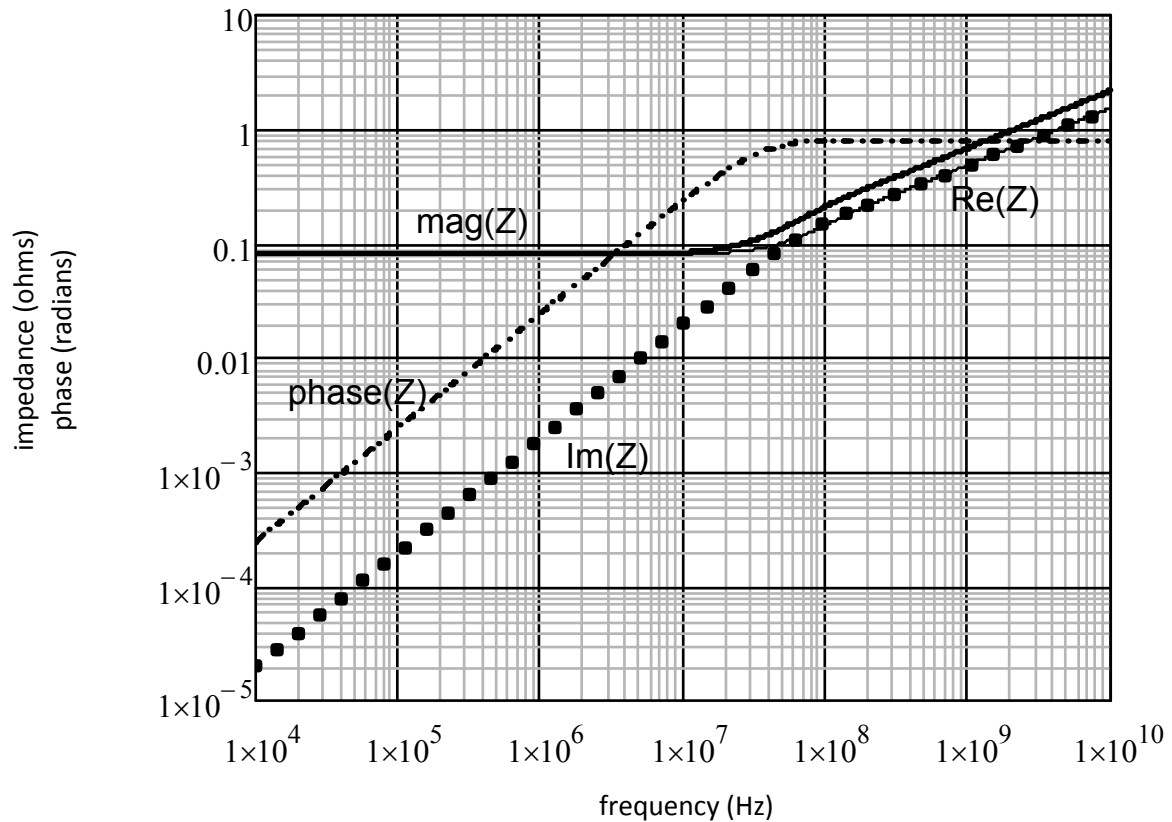


Figure 5. Internal Impedance of a 10m Long 1" Radius 36AWG Copper Wire Braid Coaxial Shield²

2.1.2.3. Ramo, Whinnery, & Van Duzer, Internal Inductance³

The energy method³ derives the inductance from the stored magnetic energy,

$$(25) \quad \frac{1}{2} \cdot L_{int} \cdot I^* \cdot I = \frac{1}{2} \cdot \iiint \vec{B} \cdot \vec{H} \cdot dV.$$

For a cylindrical shell of outer radius, c , inner radius, b , and length, l , this method results in

$$(26) \quad L_{int} \cong \frac{\mu_0 \cdot l}{2 \cdot \pi \cdot (c^2 - b^2)^2} \cdot \left[\frac{c^4 - b^4}{4} - b^2 \cdot (c^2 - b^2) + b^4 \cdot \ln\left(\frac{c}{b}\right) \right].$$

This result does not agree with Schelkunoff's dynamic solution to the boundary problem.

In the energy method of Ramo, et al, above, their estimate of the magnetic field inside a conducting cylinder with a constant current density is as follows:

$$(27) \quad H_{\phi}(r) \cong \frac{I \cdot r}{2 \cdot \pi \cdot a^2}.$$

In the solution to the dynamic boundary value problem, also from Ramo, et al, the magnetic field inside the same conducting cylinder is as follows:

$$(28) \quad H_{\phi}(r) = \frac{\sigma \cdot E}{k} \cdot \frac{I_0(k \cdot r)}{J_0(k \cdot a)}, \text{ where } a \text{ is the cylinder outer radius and}$$

$$(29) \quad k \cong \sqrt{i\omega \cdot \mu \cdot \sigma}.$$

The two methods agree for a solid cylinder.

2.2. External and Mutual Inductance³

External inductance exists when magnetic fields from a current carrying conductor interact with another conductor, either the same conductor looping back on itself forming a closed circuit or with another such nearby closed circuit. This is necessary for integral form of Ampere's law to be non-zero. The magnetic field, $H(r)$, generated by a loop of current, $I(r')$, is as follows:

$$(30) \quad H(\vec{r}) = \oint \frac{I(\vec{r}') d\vec{l} \times (\vec{r} - \vec{r}')}{4\pi \cdot |\vec{r} - \vec{r}'|^2}.$$

Kirchhoff's Voltage Law requires the sum of all voltages around the circuit loop to be zero. Ignoring capacitive effects, that means that the resistive component of the voltage drop around the loop plus the inductive component of the voltage drop around the circuit must add up to the voltage source creating the current.

$$(31) \quad V_{total} + V_R + V_L = 0, \text{ or}$$

$$(32) \quad V = R \cdot I + L \cdot \frac{dI}{dt}, \text{ where}$$

the resistance, R , of a conducting element is related to the conductivity, σ , and the geometry of that element, length, l , and cross section area, A ,

$$(33) \quad V_R = -\int \frac{\vec{j} \cdot d\vec{l}}{\sigma} = -\int \frac{I \cdot d\vec{l}}{\sigma \cdot A} = -I \cdot R \text{ and}$$

the external inductance is derived from

$$(34) \quad V_L = -\frac{\partial}{\partial t} \iint \vec{B} \cdot d\vec{A} = -\frac{\iint \vec{B} \cdot d\vec{A}}{I} \cdot \frac{dI}{dt} = -L_{ext} \cdot \frac{dI}{dt}, \text{ where}$$

$$(35) \quad L_{ext} = \frac{1}{I} \cdot \iint \vec{B} \cdot d\vec{A}.$$

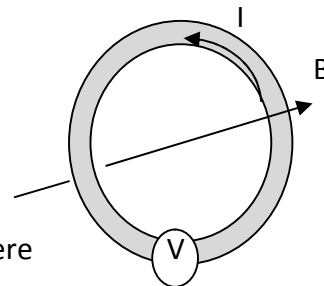


Figure 11. Conducting Loop

This last formulation is called the flux-linkage method for deriving external inductance. Mutual inductance, M_{12} , between two circuits, 1 and 2, derives the same except that the current in circuit #1 is driving a voltage in circuit #2:

$$(36) \quad M_{12} = \frac{1}{I_1} \iint \vec{B}_1 \cdot d\vec{A}_2.$$

The internal inductance, L_{int} , is added to the external inductance to complete the inductance model.

A cylinder of length, l , radius r , and a height, h , above a groundplane has an external inductance

$$(37) \quad L_{external} \cong \frac{\mu_0 \cdot l}{2 \cdot \pi} \cdot \ln\left(\frac{2 \cdot h}{r}\right).$$

The internal inductance that is so much smaller that we always ignore its existence and lose sight of its significance until we have a special case where the circuit doesn't close on itself.

Table 1. System & Cable Parameters used in Model Calculations

	length	radius	thickness	conductivity	L_{int}	L_{ext}	R_{dc}
CFC Composite	10m	2m	2mm	$10^4 S/m$	1nH	524nH	80m Ω
¼" 40AWG wire braid	10m	1/8"	$8 \cdot 10^{-5} m$	$5.8 \cdot 10^7 S/m$	25nH	12 μ H	127m Ω

The difference in external inductance creates WF5A in present-day ground tests with their nearby return current flowing back to the pulse generator.

2.3. Inductance Comparisons

A 10m cable with a 1' diameter, 3" above a groundplane, has an external inductance of 497nH/m or 5 μ H for the 10m length.

If the same cable is a 36AWG wire braid and is isolated from any groundplane or another conductor, its internal inductance is 40nH/m or 400nH for the 10m length.

A 10m long, 2m diameter, 2mm thick CFC cylinder in a coaxial test fixture with of 6m diameter will have an external inductance of 200nH/m or 2 μ H for the 10m length.

A 10m long, 2m diameter, 2mm thick CFC cylinder has an internal inductance of 100pH/m or 1nH for the 10m length.

We are dealing with two to three orders of magnitude difference between external and internal inductance of common cylindrical conductors in aircraft, the skin, cable shields, and plumbing.

*The author thanks Roxanne Arellano for many hours discussing this illusive subject that even our references do not agree upon.

3. Official Indirect Lightning Waveforms^{4,5}

Direct lightning strike waveshapes are broken down to Components A through H. Indirect lightning is asked to respond only to Components A, D, and H. Indirect lightning waveshapes are broken down to Waveforms 1 through 6 and should include more.

For reference in the rest of the discussion, all of the SAE ARP5412A indirect lightning waveforms mathematical expressions are listed in Table 2, below, and graphed in Figure 12, below. Section 2.1.1 and 2.1.2 of paper #3 show the physics and math derivations of the standard waveforms.

Table 2. Indirect Lightning Waveforms extracted from SAE ARP5412A Table 9⁴

- Component A and Waveforms 1 and 4 are the same 1.5 μ s/88 μ s double exponential with a x1.094 multiplier, i.e. $I_A(t) = 200kA \cdot 1.094 \cdot (e^{-t/88\mu s} - e^{-t/1.5\mu s})$ peaks at 200kA.
- Waveform 2 is the derivative of Waveform 1 (and A and 4) with a x1.00 multiplier. (Actually, WF2 does not graph simply as the derivative of WF4, but does graph nicely as $WF2(t) \cong -A \cdot e^{-t/100ns} + B \cdot e^{-t/1.5\mu s} - C \cdot e^{-t/88\mu s}$, give or take whatever is agreed to be the rise time, in this case, 100ns.)
- Waveform 3 is a damped sinusoid waveform at 1 and 10MHZ with a damping Q-value of 9-37 with a x1.059 multiplier. Actually, aluminum skinned vehicles have $Q \leq 20$ and cables have $Q \leq 10$.
- Waveform 5 consists of two waveforms, 5A the current on cables in CFC airframes in ground test:
 - Waveform 5A is a 23 μ s/79 μ s double exponential with a x2.334 multiplier.
 - Waveform 5B is a 12.5 μ s/631 μ s double exponential with a x1.104 multiplier.
- Missing is the waveform that follows Component D, a 772ns/44 μ s double exponential.
- Waveform 6_H follows Component H, a 52ns/53 μ s double exponential.

Indirect Lightning Waveforms

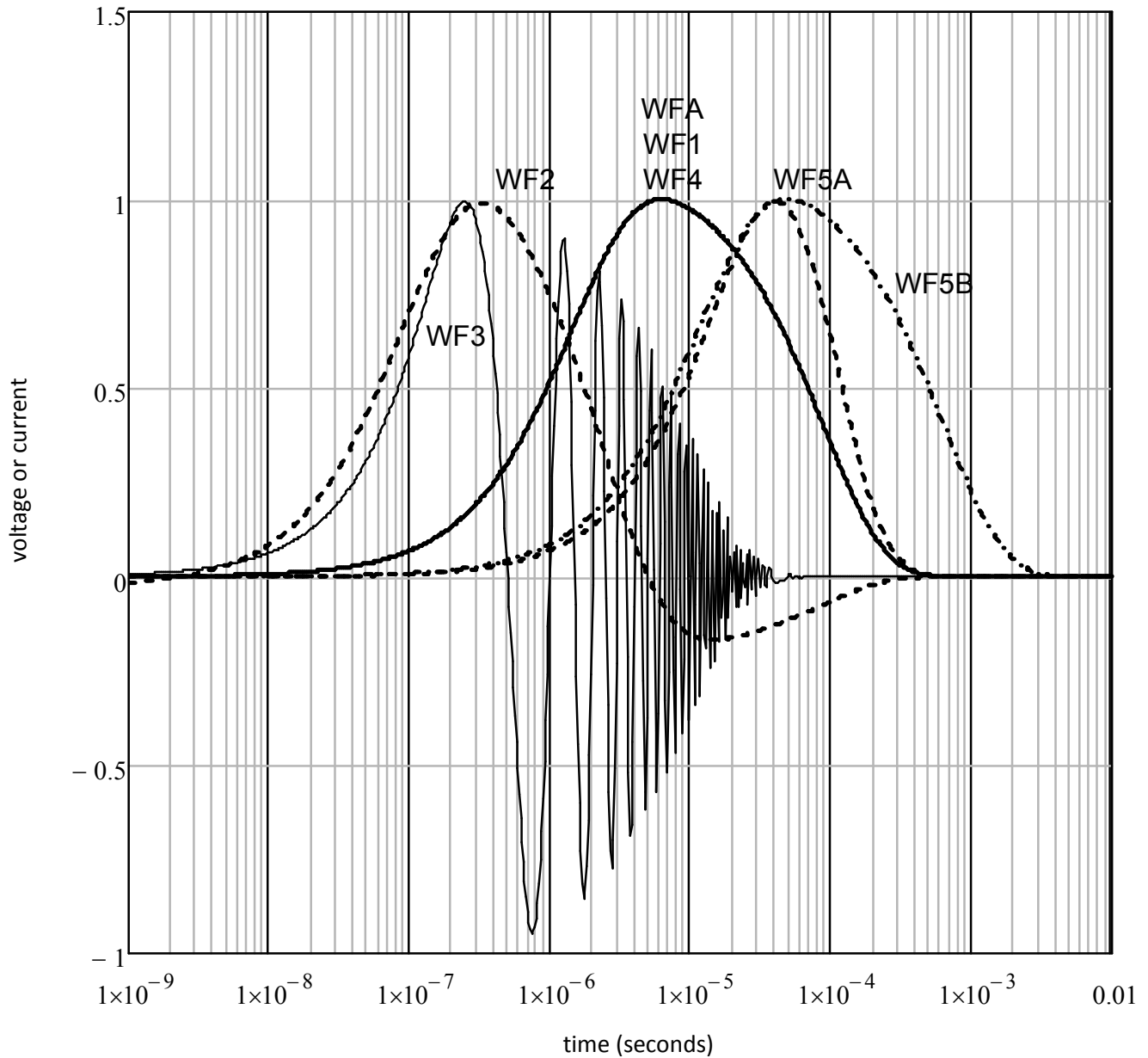


Figure 12. Indirect Lightning Waveforms 1, 2, 3, 4, 5A & 5B

4. Comparison of Component A Induced Currents, In Flight & Ground Test

Most CFC laminates used in aircraft skins have thicknesses ranging from 0.5mm to 6mm.⁹ The thinner skins are used in sandwich constructions with Kevlar or metal honeycomb in the middle for strength. Table 1 lists the parameters used in this example calculation.

Lightning strike zones on the exterior affect the nature of the induced indirect lightning transients on the interior wiring. To quote (and embellish) SAE ARP5415A, 4.4.1: "Since most aircraft systems are installed in airframe sections that do indeed lie between Zone 1A (first return stroke zone or initial attachment) or 1B (first return stroke zone with long attachment or the discharge region) attachment

zones or within an associated Zone 3 (current conduct zone in between initial attachment and discharge zones), this usually exposes all system installations to current Component A and the total multiple stroke and multiple burst waveform sets.”¹² With that, we will analyze the I-R-drop effects of lightning Component A, multiple stroke Component D, and multiple burst Component H waveforms.

The lightning Component A is defined as follows:⁴

$$(38) \quad I_A(t) = I_A \cdot (e^{-\alpha \cdot t} - e^{-\beta \cdot t}), \text{ where}$$

$$(39) \quad I_A = 218 \text{ kA},$$

$$(40) \quad \alpha = 1/88 \mu\text{s}, \text{ and}$$

$$(41) \quad \beta = 1/1.5 \mu\text{s}$$

in order to produce the peak 200kA lightning criterion.

The voltage induced across the parallel RL circuit is as follows in terms of the Laplace frequency, s :¹

$$(42) \quad V_{RL}(s) = I_A(s) \cdot \frac{Z_{CFC}(s) \cdot Z_{cable}(s)}{Z_{CFC}(s) + Z_{cable}(s)}, \text{ where}$$

$$(43) \quad I_A(s) = I_A \cdot \left(\frac{1}{s+\alpha} - \frac{1}{s+\beta} \right),$$

$$(44) \quad Z_{CFC}(s) \cong R_{CFC} + s \cdot L_{CFC} = L_{CFC} \cdot (s + \alpha), \text{ where}$$

$$(45) \quad \alpha \equiv \frac{R_{dc}}{L_{dc}} \text{ is the radian frequency constant of the CFC skin,}$$

$$(46) \quad Z_{cable}(s) \cong R_{cable} + s \cdot L_{cable} = L_{cable} \cdot (s + b), \text{ where}$$

$$(47) \quad b \equiv \frac{R_{cable}}{L_{cable}} \text{ is the radian frequency constant of the cable.}$$

The CFC current is the voltage, above, divided by the CFC impedance and the cable current is the voltage, above divided by the cable impedance.

The cable current in the Laplace frequency domain is as follows:¹

$$(48) \quad I_{cable}(s) = I_A \cdot \frac{L_{CFC} \cdot L_{cable}}{L_{CFC} + L_{cable}} \cdot \left(\frac{1}{s+\alpha} - \frac{1}{s+\beta} \right) \cdot \frac{s+\alpha}{(s+\gamma)}, \text{ where}$$

$$(49) \quad \gamma = \frac{R_{CFC} + R_{cable}}{L_{CFC} + L_{cable}}$$

is the loop R/L radian frequency constant.

The time domain expression for the cable current is then as follows using Laplace tables:^{1,10}

$$(50) \quad I_{cable}(t) = I_A \cdot \frac{L_{CFC}}{L_{CFC} + L_{cable}} \cdot \left\{ \frac{(a-\alpha) \cdot e^{-\alpha \cdot t} - (a-\gamma) \cdot e^{-\gamma \cdot t}}{\gamma - \alpha} + \frac{(a-\beta) \cdot e^{-\beta \cdot t} - (a-\gamma) \cdot e^{-\gamma \cdot t}}{\gamma - \beta} \right\}.$$

A similar process yields the expression for the current on the CFC skin.

$$(51) \quad I_{CFC}(t) = I_A \cdot \frac{L_{cable}}{L_{CFC} + L_{cable}} \cdot \left\{ \frac{(b-\alpha) \cdot e^{-\alpha \cdot t} - (b-\gamma) \cdot e^{-\gamma \cdot t}}{\gamma - \alpha} + \frac{(b-\beta) \cdot e^{-\beta \cdot t} - (b-\gamma) \cdot e^{-\gamma \cdot t}}{\gamma - \beta} \right\}$$

The loop frequency constant, γ , plays an important role in controlling the induced currents through the different impedances, both cable and CFC skin, now including internal inductances in-flight and external inductances in ground tests.

The following two example calculations used ten twisted shielded pairs (TSP), 1/4" in diameter with 40AWG wire braid, 10m long. This was done to illustrate the extreme currents carried internally to a CFC composite airframe. The first example, Figure 13, is the in-flight case with internal inductances and the second example, Figure 14, is the ground-test case with external inductances, all itemized in Table 2. The only difference between the two figures is the inductance of the conductors.

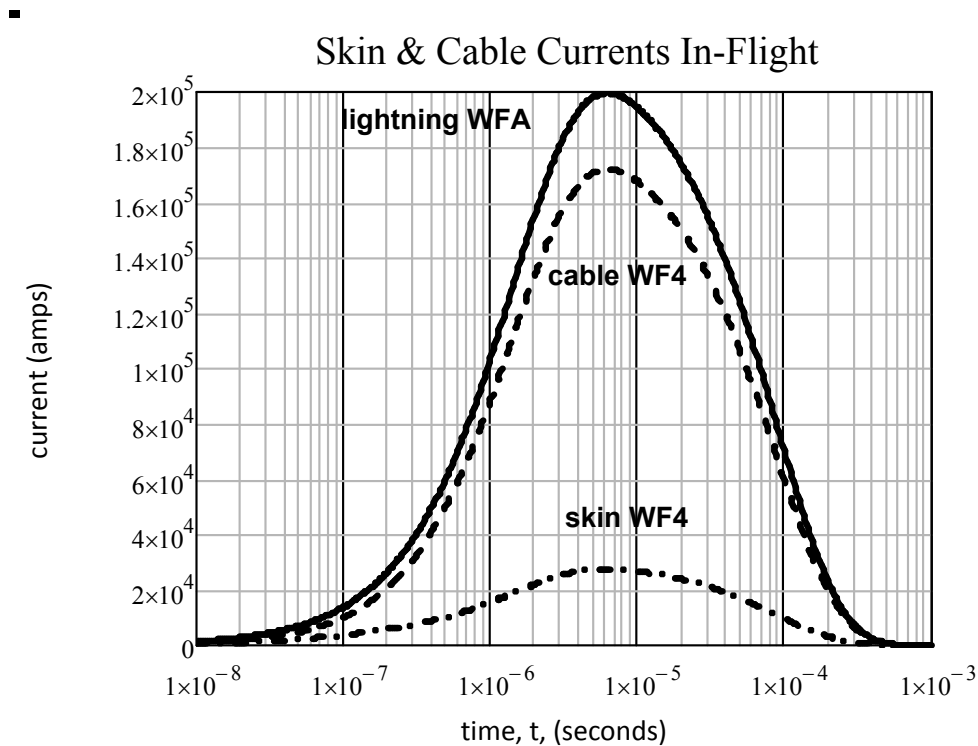


Figure 13. In-Flight Lightning Stroke WFA plus Induced Current on Ten Cables and the CFC Skin

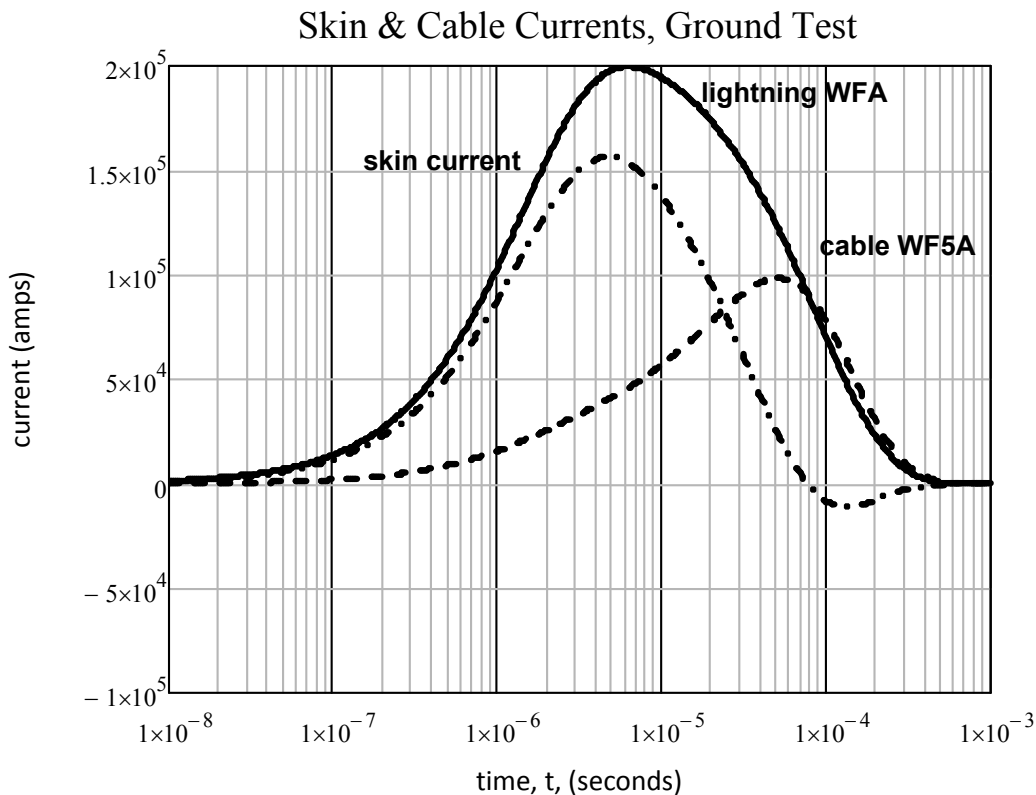


Figure 14. Ground Test Lightning Stroke WFA plus Induced Current on ten Cables and the CFC Skin

The in-flight internal/self inductance is too low to alter the current division; it is almost entirely current division by the resistance of the parallel components.

Both the in-flight skin current and cable current follow WF4, the same as the lightning stroke Component A.

The WF5A cable current is entirely a product of ground testing with a nearby current return path.

Bottom line: The major difference between in-flight and ground test is the cable current waveform with about a 30% increase in peak current and a 120% increase in rise time. More current is on the in-flight cable because the lower cable inductance is not diverting it to the skin. The current division in-flight is mostly resistive.

5. Multiple Stroke Component D Induced Currents, In Flight

Multiple stroke strikes are defined as one Component D strike with a peak of 100kA followed by thirteen strikes at one half the Component D amplitude with 10ms to 200ms between strikes distributed over a time of 1.5s.

The Component D waveform is defined as follows:⁴

$$(52) \quad I_D(t) = 109.405kA \cdot (e^{-t/44\mu s} - e^{-t/773ns})$$

This current divides between the skin and internal conductors as shown below in Figure 15. The faster rise time is not affected by the internal inductance any more than the slower Component A in Figure 7.

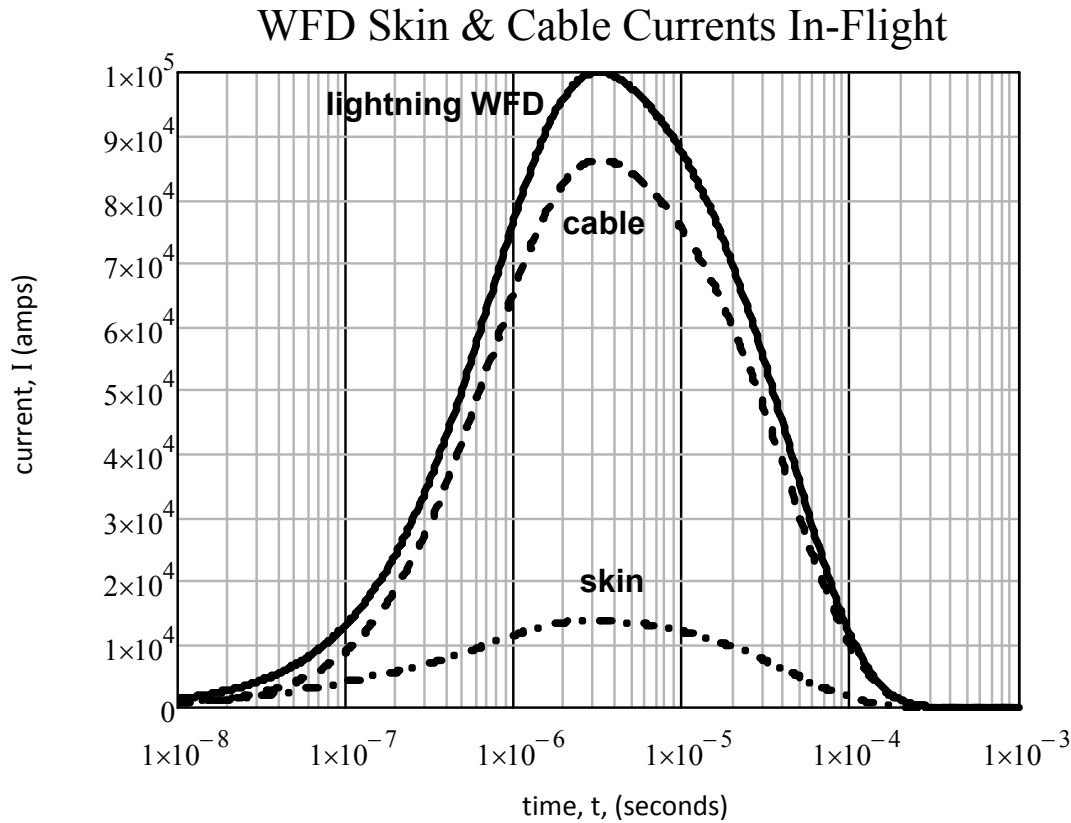


Figure 15. Component D Current Division between CFC Skin & Ten Cables

SAE ARP5412A does not include an indirect lightning waveform following the Component D waveform however when it does, the above model demonstrates that these cable current amplitudes can reach about 885kA in amplitude. 5412A does include the following Table 3 of indirect waveforms attributable to Component D.

Table 3. SAE ARP5412A Indirect Lightning Responses to Multiple Strike Component D

SAE ARP5412A Table 4 – Response to D and D/2 as a Fraction in Response to A					
Response	WF1	WF2	WF3	WF4	WF5
to D	1/2	1	1	1/2	2/5
to D/2	1/4	1/2	1/2	1/4	1/5

The table erroneously attributes Waveforms 4 and 5A to Component D strikes whereas in fact they can only come from Component A waveform. Component D current on a CFC skin can be attenuated and its rise time increased until it looks almost like WF4 depending upon entry and exit points and swept stroke attachment points. However, it can enter the interior directly with its own waveform. WF2 and WF3, above, are OK as will be shown below in Section 7.

6. Multi-Burst Component H Induced Currents, In Flight⁴

Multi-burst strikes are defined as 3 bursts of 20 Component H transients, 50 μ s-1ms between individual transients, 30ms-300ms between bursts, not to exceed 620ms in total duration.

The Component H waveform is defined as follows:

$$(53) \quad I_H(t) = 10.572kA \cdot (e^{-t/53\mu s} - e^{-t/52ms})$$

This current divides between the skin and internal conductors as shown below in Figure 16. The faster rise time is likewise not affected by the internal inductance any more than the slower Component A in Figure 13 and Component D in Figure 15 depending upon entry and exit points.

■

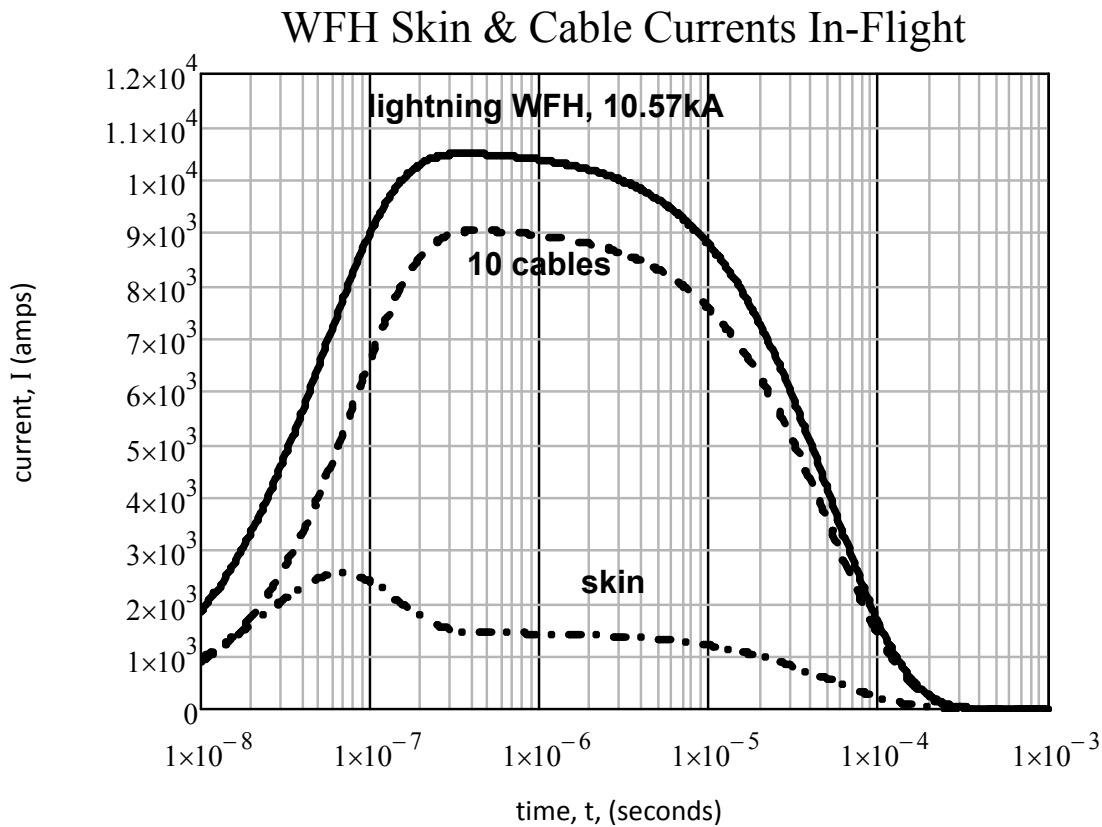


Figure 16. Waveform H Current Division between CFC Skin & Ten Cables

SAE ARP5412A has an indirect lightning Waveform 6H due to a Component H strike defined as follows with the same waveform:

$$(54) \quad I_{6H}(t) \equiv I_{6H} \cdot (e^{-t/52ms} - e^{-t/53\mu s}),$$

$$(55) \quad I_{6H} = 6-160A$$

The in-flight model herein concludes that I-R-drop cable currents following Component H waveform can reach 900A in amplitude, 15dB larger than the above level. Component D current on a CFC skin

may be attenuated and its rise time increased until it looks almost like Waveform 4 depending upon entry and exit points and swept stroke attachment points.

7. Waveforms 2 & 3

Components a, D, and H have the same peak di/dt and the same spectral content above 2MHz. The spectra of Components A, D, and H are plotted in Figure 17. Clearly, in terms of frequency content, Components D and H are comparable to Component A above 1.5MHz. This makes typical WF3 damped sinusoid system and cable resonances comparable for all three since such small differences are insignificant at this level of system application. SAE ARP5412A erroneously has WF3 from Component D 40% smaller than that from Component A.

Comment: These waveforms are simplistic mathematical models whose higher frequency content derives more from the discontinuities in the models at $t = 0$ than from the physics of lightning. Drawing the curves with too fine a line width is self deceiving.

■

Lightning Spectra A, D, & H

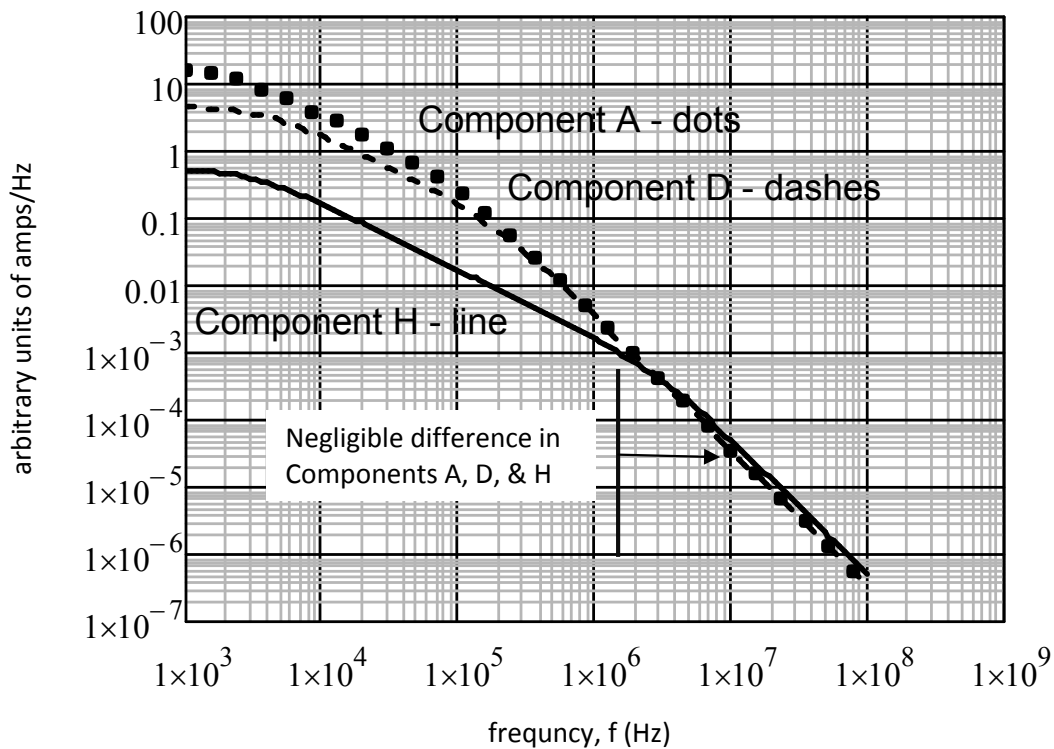


Figure 17. Spectra of Lightning Components A, D, & H

Damped sinusoid resonant frequencies are inversely proportional to the lengths of the system and cables and, more often than not, depend upon system and cable lengths approximately as half-wavelength resonant lines. Their amplitudes are proportional to length.

$$(56) \quad f_{res} \approx c/2 \cdot l,$$

where l = system or cable length, c = speed of light or $3 \cdot 10^8$ m/s.

Waveform 2 peak currents have the same property. Taking the derivative of Components A, D, and H by approximating them as their peak levels divided by their respective rise-times results in the following:

$$(57) \quad \dot{I}_A(\text{WF2 peak}) \cong 1.5 \cdot 10^{11} \text{ A/s}$$

$$(58) \quad \dot{I}_D(\text{WF2 peak}) \cong 1.4 \cdot 10^{11} \text{ A/s}$$

$$(59) \quad \dot{I}_H(\text{WF2 peak}) \cong 2.1 \cdot 10^{11} \text{ A/s}$$

These are within 33% of each other and, in fact, are the same as their spectra at the second break frequency. The high frequency in these model waveforms is due more to the discontinuities in the waveforms at $t = 0$ than to the physics of lightning therefore these small differences, above, should be considered irrelevant and we should settle on one value for all, say, $2 \cdot 10^{11} \text{ A/s}$. These WF2 currents are the source terms for induced voltages, $V = A \cdot dB/dt$.

8. Summary and Impact

8.1. Summary

- All design allocations and box testing that heretofore called out WF5A from a Component A strike in composite airframes will have to be changed to WF4 with appropriate amplitude corrections.^{4,5,12}
- System level test results containing WF5A cable currents will have to be ignored for certification purposes. The results can be used for model verification and checking groundplane and cable shield integrity.^{4,5,12}
- Shielding the WF4 current has the same problems as WF5A since WF5A is the late time low frequency portion of WF4/WFA.¹ A revision of IN608, IN616, will explain the differences.
- Components D and H will induce I-R-drop voltage and current waveforms that can be confused for WF4 depending upon entry and exit points and the CFC thickness. If they contact components on the exterior connected to the internal cables and/or groundplane(s), they will conduct through the interior with their own waveforms. If they do not contact components connected to the interior, they will diffuse through the CFC skin with slower rise times and waveforms that can be confused for WF4 although probably never be the same as WF4. WF5A currents can only exist in present-day ground-tests.
- Components A, D, and H excite the same peak levels of WF2 and WF3.
- Certification will take more analyses than normally desired until the system test and box tests are corrected. The relationship between cable currents in ground tests and those in-flight has to be resolved by analysis until a credible system level test is designed. There are more detailed changes as a result of the investigation herein but they will be enumerated in later notes for that purpose.
- A new system level lightning test technique is needed to eliminate the effects of the return current in present day tests.¹³

8.2. Impact of Changes

A natural question to ask after years of certifying to cable current WF5A instead of WF4 is what is the difference?

(a) The in-flight cable current is about 30% larger (in the example above) and the rise time is x12 times faster. That produces more high frequency content and larger inductive coupling. The amplitude and derivative effects combined are approximately 24dB increase in inductively coupled transients' peak amplitude thereby increasing mutual coupling to less exposed cables. Component ratings for peak power may be affected.

(b) The effects on susceptibilities are more difficult to define. The combined effects can only lower thresholds but how much requires experimental study. Systems certified to WF5A have lower safety margins.

(c) The skin current decreases by as much as x5 or 14dB therefore inductive coupling through apertures decreases. Inductive coupling between interior cables increases due to faster rise times.

(d) More theoretical and experimental work is needed and each system has to be analyzed with its own characteristics. "One size does not fit all."

References

1. West, Larry, Interaction Note 608, "Lightning Induced Waveform 5 in Composite Airframes, the Inability of Copper Braid to Shield It, and A New Layered Copper Braid and High- μ Foil Shield", February 2009, www.ece.unm.edu/summa/notes/ln/0608.pdf, Revision A, Paper #3, April 2011
2. Schelkunoff, S. A., "The Electromagnetic Theory of Coaxial Transmission Lines and Cylindrical Shields", The Bell System Technical Journal, Volume XIII, 1934, 532-579
3. Ramo, Whinnery, & Van Duzer, *Fields and Waves in Communication Electronics*, 3rd Edition, John Wiley & Sons, NY, 1994
4. Society of Automotive Engineers Aerospace Recommended Practices, SAE ARP5412A, "Aircraft Lightning Environment and Related Test Waveforms", Revised 2005-02
5. Radio Technical Committee on Aeronautics, RTCA/DO-160F, "Environmental Conditions and Test Procedures for Airborne Equipment, Section 22, Lightning Induced Transient Susceptibility", 2007-12
6. Rosa and Grover, "Formulas and Tables for the Calculation of Mutual and Self Inductance", Bureau of Standards Bulletin, Vol. 8, No. 1, 1912
7. Rosa, Edward G., "The Self and Mutual Inductances of Linear Conductors", Bulletin of the Bureau of Standards, Vol. 4, No. 2, 1908, p 301-344, <http://www.g3ynh.info/zdocs/refs/NBS/Rosa1908.pdf>
8. Grover, Frederick W., *Inductance Calculations*, Dover Publications Inc., NY, 2009 (copyright 1949)
9. Baldacim, Crisofani, & Lautenschlager, "Lightning Effects in Aircraft of the Composite Material", 17th CBECIMat – Congresso Brasileiro de Engenharia e Ciência das Materials, 15 a 19 de Novembro de 2006
10. Goldman, Stanford, *Laplace Transform Theory and Electrical Transients*, Dover Publications, Inc., NY, 1966 (copyright 1949)
11. Lee, K. S. H., Editor, *EMP Interaction: Principles, Techniques, and Reference Data*, Taylor & Francis, NY, 1995, a summary reference book based mostly on the Note Series of Carl E. Baum
12. SAE ARP 5415A, "User's Manual for Certification of Aircraft Electrical/Electronic Systems for the Indirect Effects of Lightning", Revised 2002-04
13. West, Larry, *Indirect Lightning in Composite Aircraft*, Self Published Public Domain, TX, 2011